nature physics

Article https://doi.org/10.1038/s41567-023-02142-z

A thermodynamic explanation of the Invar effect

In the format provided by the authors and unedited

Supplementary Information: A thermodynamic explanation of the Invar effect

S. H. Lohaus,[1] M. Heine,[2] P. Guzman,[1] C. M. Bernal-Choban,[1] C. N. Saunders,[1] G. Shen,[3] O. Hellman,[4] D. Broido,[2] and B. Fultz[1]

[1] *Dept. of Applied Physics and Materials Science, California Institute of Technology, Pasadena, CA 91125, USA*

[2] *Dept. of Physics, Boston College, Chestnut Hill, MA 02467, USA*

[3] *Advanced Photon Source, Argonne National Laboratory, Argonne, IL 60439, USA*

[4] *Dept. of Molecular Chemistry and Materials Science, Weizmann Institute of Science, Rehovoth 76100, Israel*

(Dated: May 31, 2023)

This Supplementary Information presents data and analyses of (a) lattice parameter and thermal expansion from synchrotron X-ray diffraction, (b) time spectra from nuclear forward scattering and hyperfine magnetic field distributions obtained from them, (c) heat capacity measurements and an assessment of the magnetic entropy, (d) phonon partial DOS curves of Fe and Ni, obtained from computation and from the joint analysis of neutron and NRIXS spectra.

A. Lattice Parameter and Thermal Expansion

The lattice parameter of $Fe_{65}Ni_{35}$ was measured as a function of pressure at two temperatures (295 K and 390 K) as described in the Methods. Fig. S1 shows that below 3 GPa the lattice parameter of Invar is the same for both temperatures, so there is no detectable thermal expansion between room temperature and 390 K (see insert). Above the Curie transition the volume increases with temperature, and the thermal expansion takes a more typical value of $\beta = 3.4 \cdot 10^{-5}\ \mathrm{K}^{-1}$. To our knowledge, these are the first direct measurements of the thermal expansion of $Fe_{65}Ni_{35}$ as a function of pressure.

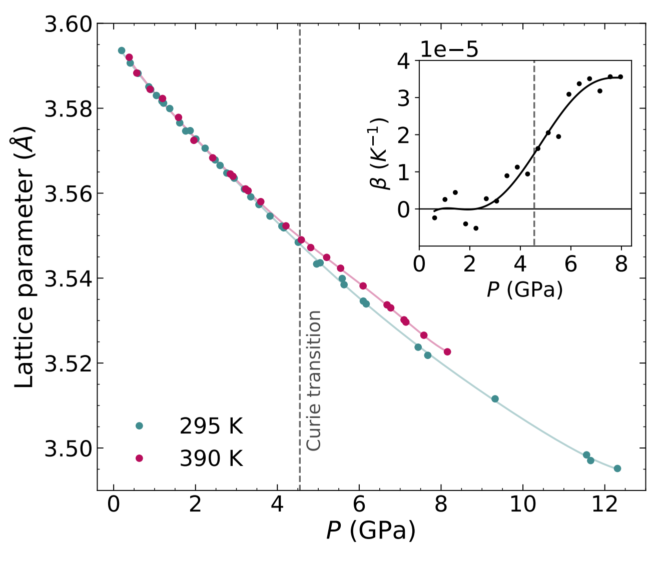

FIG. S1. Lattice parameter and thermal expansion of Invar as a function of pressure. Lattice parameter vs. pressure were measured by synchrotron X-ray diffraction at two temperatures, with samples inside diamond anvil cells. The insert shows the volumetric thermal expansion coefficient β from these data. Solid lines are polynomial fits.

B. NFS spectra

Nuclear forward scattering (NFS) measures temporal interference patterns of photons emitted as ^{57}Fe nuclei make transitions back to their ground states after being excited by a synchrotron flash. Magnetism causes a nuclear Zeeman splitting of the hyperfine levels, and transitions from different hyperfine energy levels give rise to interference beats in the NFS spectra. The measured magnetic beat patterns (intensity modulations) can be fitted to a distribution $P(B_{hf})$ of hyperfine magnetic fields (HMF). Figure S2 shows the evolution of the NFS spectra and their fits as the magnetic beat patterns are changed under pressure. The spectra were fitted to extract the HMF distributions $P(B_{hf})$ shown in Fig. S3. The magnetization $M(P)$ presented in Fig. 3 of the main manuscript is the normalized mean of these HMF distributions.

At low pressures, the pronounced magnetic beats of Fig. S2 correspond to a near-ferromagnetic state. The beats broaden with increasing pressure, and the spectrum at 4.4 GPa shows an almost exponential decay, consistent with a near-paramagnetic state. The decrease in magnetization within this region is shown in Fig. S3 as the HMF distributions move toward lower fields with increasing pressure.

The broad beats in the NFS spectra above 4.6 GPa (Fig. S2) are nearly independent of pressure. They originate from the sample thickness, where photons emitted at different depths interfere with each other. We therefore fitted the spectra above the Curie transition with a superposition of paramagnetic patterns for two sample thicknesses that are close to the nominal thickness of our samples. Nevertheless, since the time window of these measurement (about 110 ns) is constrained by the bunch spacing in the APS storage ring, the fits cannot reliably distinguish this thickness effect from beats from a small magnetic field. Fortunately this does not affect the results for the magnetic entropy below the Curie transition that is presented in the main manuscript. A previous

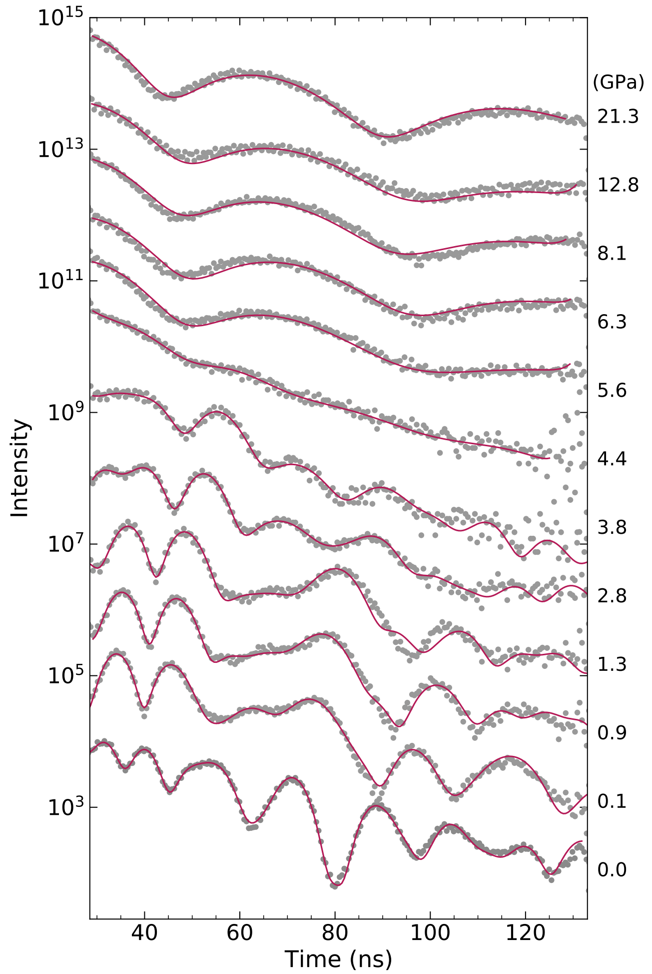

FIG. S2. NFS spectra of Invar at labeled pressures. Solid lines are the fits used to extract the HMF distributions.

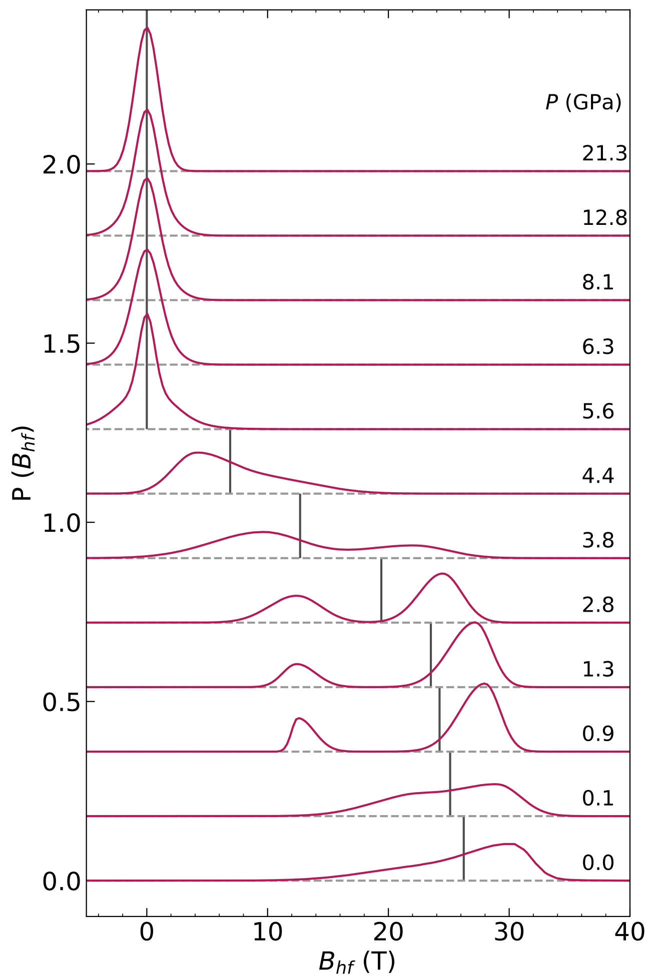

FIG. S3. Hyperfine magnetic field (HMF) distributions of Invar at different pressures. The distribution $P(B_{\mathrm{hf}})$ was found by fitting the NFS data of Fig. S2. The fitted HMF distributions consist of two asymmetrized Gaussians. Vertical lines mark the mean of each distribution.

conventional Mössbauer spectrometry measurements on Invar alloys containing ^{57}Co radioisotope [1], showed that the magnetization and HMF go to zero at a Curie transition in pressure.

For calculating the magnetic entropy of Fig. 4a of the main manuscript, we use the magnetization normalized at ambient conditions up to the Curie transition from the NFS experiments. The total entropy at the Curie transition is calibrated by the heat capacity measurements (see Eq. 6 of the main manuscript). In reality $M < 1$ at ambient conditions, however our computed entropy is nearly unaffected by this. If, instead, the magnetization is normalized with data taken at 20 K (not shown here), only the curvature of the entropy has a minor increase, but its total change up to the Curie transition is exactly same because it is calibrated by heat capacity. See [2] for this alternative analysis.

C. Heat Capacity

The heat capacity of Invar was measured by differential scanning calorimetry (DSC) from room temperature to 773 K, and is displayed in Fig. S4a. These measurements are in good agreement with [3, 4]. The phonon contribution to the heat capacity was calculated using the measured phonon DOS, $g(\varepsilon)$, as [6]:

$$C_{P,\mathrm{ph}}(T) = 3N\,k_{\mathrm{B}} \int_0^{\infty} g(\varepsilon) \;\left(\frac{\varepsilon}{k_{\mathrm{B}}T}\right)^2 \times \;\frac{\mathrm{e}^{\varepsilon/k_{\mathrm{B}}T}}{\left(\mathrm{e}^{\varepsilon/k_{\mathrm{B}}T}-1\right)^2}\,\mathrm{d}\varepsilon \quad (1)$$

where ε is the phonon energy and $n_{\varepsilon,T} = (\exp(\varepsilon/k_{\mathrm{B}}T) - 1)^{-1}$ the Planck distribution of phonon occupancy. The remaining heat capacity comes from electrons and spins.

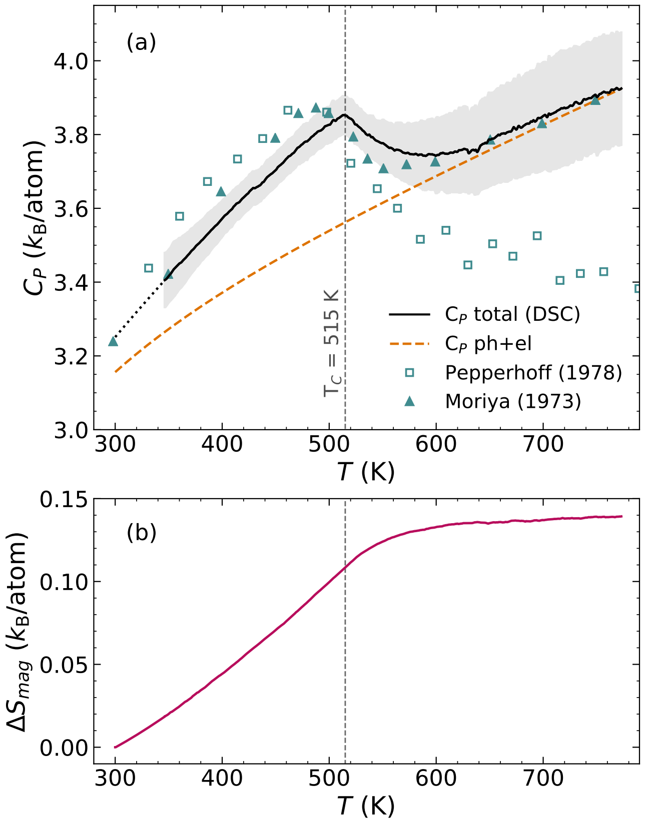

FIG. S4. Heat capacity contributions and magnetic entropy of Invar. (a) Heat capacity of Invar measured by DSC, compared to labeled references. Dashed curve shows the phonon contribution (measured by NRIXS) together with the electronic heat capacity (fitted at high temperatures). Gray errors show the standard deviation of three sequential DSC measurements on two different samples (see Methods). (b) Change in magnetic entropy above 300 K calculated with Eq. 2.

The broad magnetic transition can be clearly identified in the measured heat capacity, with a Curie transition at 515 K. Some magnetic short-range order is apparent above the Curie temperature, but above 650-700 K the heat capacity is dominated by phonons and electrons. The magnetic entropy shown in Fig.S4b was obtained as:

$$\Delta S_{\mathrm{mag}}(T > 300) = \int_{300\mathrm{K}}^{T} \frac{C_{P,\mathrm{mag}}(T')}{T'} dT' \qquad (2)$$

The change in magnetic entropy between RT and the Curie transition is $\Delta S_{\mathrm{mag}}(T_{\mathrm{C}}) = 0.11 \pm 0.005 k_{\mathrm{B}}$/atom, where the uncertainty was propagated from errors in the calorimetry measurements.

D. Partial Phonon DOS

NRIXS is a resonant technique that measures the partial phonon density of states (DOS) of ^{57}Fe in the material. The partial phonon DOS from Fe and Ni atoms in fcc alloys were previously shown to be very similar [5], which is not surprising due to their similar masses and electron configurations. Calculations are able to compute individual DOS contributions from Fe and Ni to the total phonon DOS of $Fe_{65}Ni_{35}$ Invar. Figure S5a shows those calculations at ambient pressure and temperature, confirming the similar contributions from Fe and Ni to the phonon DOS spectrum.

In addition to NRIXS, we also measured the phonon spectrum of Invar with inelastic neutron scattering (INS) at ambient conditions, for which Ni has about a 50% larger scattering cross-section than Fe. Combining NRIXS with INS, and accounting for the different weights and cross-sections, allows us to extract the partial DOS of Fe, Ni, and the total DOS shown in Fig. S5b. The experimental entropy computed from the (normalized) partial Fe DOS and from the total DOS are extremely similar (Fig. S5c), they differ by approximately 0.14%. There are minor differences around 30 meV, but when computing the total entropy by integrating the entire DOS up to 40 meV, both entropies are almost indistinguishable. The partial Fe DOS is sufficient to compute the total entropy of Invar.

[1] Rhiger, D. Mössbauer Experiments in Iron-Nickel Alloys at High Pressures. Ph.D. dissertation in physics, Univ. Washington, Seattle (1972).

[2] Lohaus, S. H. Experimental study on the thermodynamic interactions of phonons and magnetism in Fe systems. Ph.D. dissertation in Materials Science, California Institute of Technology, Pasadena (2023).

[3] Tanji, Y., Asano, H. and Moriya, H. Specific Heats of Fe-Ni (fcc) Alloys at High Temperature. *Sci. Reports Res. Institutes, Tohoku Univ.* **24**, 205 (1973).

[4] Bendick, W., Ettwig, H. H. and Pepperhoff, W. Anomalies in specific heat and thermal expansion of FCC iron alloys. *J. Phys. F: Met. Phys.* **8**, 2525 (1978).

[5] Lucas, M. S., Mauger, L., Muñoz, J. A., Halevy, I., Horwath, J., Semiatin, S. L., Leontsev, S . O., Stone, M. B., Abernathy, D. L., Xiao, Y., Chow, P and Fultz, B. Phonon densities of states of face-centered-cubic Ni-Fe alloys. *J. Appl. Phys.* **113**, 17A308 (2013).

[6] Fultz, B. *Phase Transitions in Materials, 2^{nd} ed.* Cambridge University Press, Cambridge (2020).

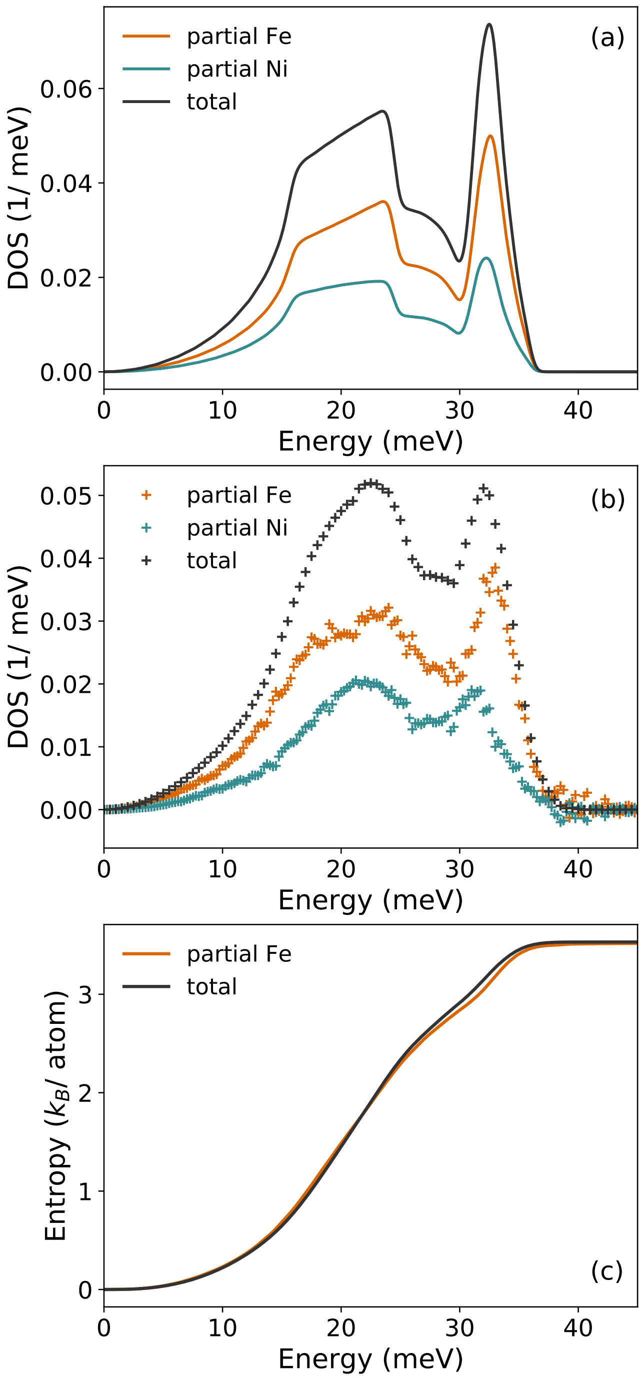

FIG. S5. Partial densities of states of Fe and Ni, their contributions to the total DOS, and effects on the phonon entropy. (a) Calculated partial phonon DOS of iron and nickel at ambient pressure and temperature. They are weighted by their atomic composition in $Fe_{65}Ni_{35}$ and add up to the total DOS of Invar. (b) Experimental partial phonon DOS of iron (from NRIXS measurements) and nickel (computed from the INS and NRIXS measurements), compared to the total DOS from INS corrected using the NRIXS measurements. (c) Cumulative experimental entropy computed from the partial iron DOS and total DOS of panel b.